Design of Inductive Power Transmission into the Rotor of an Externally Excited Synchronous Machine

Alexander Littau[1], Bernhard Wagner[1], Stefan Köhler[1], Armin Dietz[1] and Stefan Weber[2]
[1)] TH (Technische Hochschule) Georg Simon Ohm, Nuremberg, Germany
[2)] Epcos AG, Business Group Magnetics, Munich, Germany

Abstract*—Almost all drive concepts in the field of electric mobility that are currently pursued, use a permanent-magnet synchronous motor (PSM) or an asynchronous motor (ASM). The externally excited synchronous machine (EESM) type is rare, but first automotive product series exist in which the excitation power is transmitted using slip rings. On the subject of externally-excited synchronous motors, especially in combination with contactless transmission of the excitation power, there are barely any publications in the field of electric mobility. Therefore, this work, which is supported by the Bavarian Research Foundation, focuses on the research and development of a contactless system to transfer the energy needed for the external excitation on the rotor. The disadvantages of the slip ring solution in EESM are to be overcome by an inductive energy transfer to the rotor. The challenges in the design of inductive transmission is that the secondary side (rotor) rotates at high speeds in the range of 0...12000 min^{-1}, the space occupied by the energy transfer device must be kept small, the energy efficiency of the transmission has to be very high and the design needs to be very robust to meet the automotive requirements.

***Keywords*— externally excited synchronous machine, inductive energy transfer, rotating transformer**

NOMENCLATURE

A_{min}	Core cross section
A_w	Winding area
B_{max}	Magnetic flux density
δ	Air gap length
Φ_1, Φ_2	Primary and secondary flux
f	frequency
I_1, I_2	Primary and secondary current
J	Current density
k_F	Fill factor
L_1, L_2	Primary and secondary inductances
L_h	Main inductance
$L_{1\sigma}$, $L_{2\sigma}$	Primary and secondary leakage inductances
L_{h0}, $L_{1\sigma}$, $L_{2\sigma}$	Normalized inductances at one turn
N	Count of windings (turns)
P_{trans}	Transferred Power
$R_{1\delta}$, $R_{2\delta}$	magnetic air gap resistance
$R_{1\sigma}$, $R_{2\sigma}$	Magnetic leakage resistance
U_1, U_2	Primary and secondary voltage

I. INTRODUCTION

For the last years the EESM registered an increase in the market for electric vehicles [1]. This is due to the high efficiency over the whole operation range, the high start torque and the high availability of necessary materials. However, all EESMs are equipped with slip rings for feeding the excitation power. These are wear parts which have to be maintained. Furthermore they cause abrasion which deteriorates the insulation. These disadvantages should be eliminated by using contactless power transfer method instead of said slip rings.

In [2], [3] and [4] different methods are listed to excite an EESM contactlessly. However none of these meet the conditions of being highly efficient, of transmitting the necessary power level of several kW and of being compact at the same time. Therefore the aim of this work is to develop a contactless inductive energy transfer to a rotating shaft of an EESM which meets the aforementioned requirements. Furthermore, the inductive power transmitting system has to be robust and to be insensitive to the axial moving of the shaft of ±1 mm.

For this purpose, a methodology is needed that allows a fast design for different core geometries with a minimum of computational effort. In [5] and [6] a contactless power transfer via a transformer consisting of two pot cores is presented. However, this transformer type is not suitable for the usage in an EESM because the thermal tolerances of the air gap, over which the power is transmitted, are too high.

None of the methods in the mentioned contributions can be applied. Therefore, this paper pursues a different approach and presents a technique which allows rapid design with a minimum of computational effort. This paper focuses on minimum space design of the magnetic components. Furthermore, power electronics´ requirements and control design aspects are considered.

II. REQUIREMENTS

A. Subsystem

The inductive system for the contactless excitation power transmission consists of three parts: the rotating transformer, the power electronics as well as the signal analysis, control

and monitoring (Fig. 1). When designing these parts, the requirements which resulted from the EESM´s operation must be met. The relevant machine parameters can be seen in table I. At the same time it is difficult to control the high rotational speed of max. 12.000 1/min. Both the resulting centrifugal forces as well as a rotor temperature of up to 150°C, produced by the field winding must be taken into account in the calculations. Suitable construction measures have to be implemented to ensure that the components run in proper operating ranges. Furthermore, there are no sensors provided on the secondary side which constitutes a remarkable challenge for the motor control.

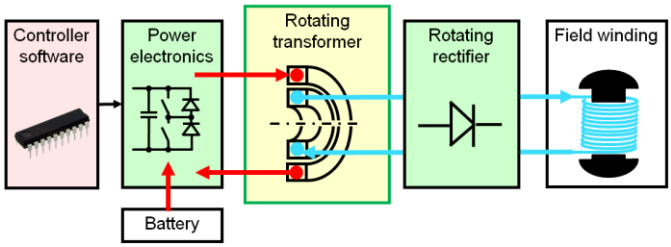

Fig. 1: Subsystem of rotary power transmission

TABLE I. PARAMETERS OF THE EESM

Nominal power	60 kW
Maximum rotating speed	12000 min^{-1}
Resistance of field winding	7 Ω
Inductance of field winding	750 mH
Maximum exciting power	2 kW
Maximum exciting current	17 A
Maximum exciting voltage	120 V

B. *Design of the rotary transformer*

The main challenges for the rotating transformer design are the control of the high centrifugal forces and the temperature on the secondary side, the package space and weight minimization as well as a high efficiency. In this case, a maximum power of 2 kW has to be transferred via air gap (see table I). On the primary side a battery-related fluctuating voltage of 220 V to 400 V is to be expected. In order to guarantee a constant power transfer there must be no change in the air gap length during the operation, which is difficult to realise due to the axial shaft movement. Therefore, core geometries have to be investigated which compensate the thermal tolerances. As these are commercially unusual, some design runs for various alternatives are necessary. For that reason a methodology was used (see Fig. 2) which allows a calculation.

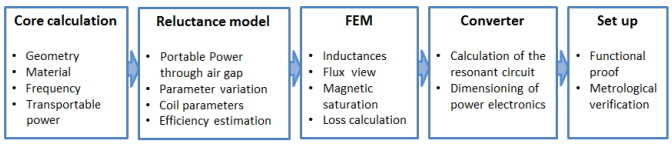

Fig. 2: Design method

The approach in designing the transformer is, after having chosen the geometry and the material, to calculate the size suitable for the core to transport the required power. Additionally, the transmitted power is estimated via the air gap with a reluctance model. In this model, the reluctance network, e.g. core-, air gap- and stray reluctances, is directly simulated with the modelica based computer software SimulationX. For an optimum transmission at this stage a first efficiency estimation and a parametric study can be performed followed by an exact calculation of inductances via FEM. Furthermore, the core´s saturation and the flow direction are displayed. As a result, it is possible to identify and avoid eddy current losses due to scattering in closer case parts. With the calculated inductors the design of a converter is following, which is supposed to achieve a maximum transmission rate, finished by metrological functions´ detection and a verification of the calculations.

C. *Power Electronics Topology and Design Aspects*

There are many requirements for the power electronics design of the inductive power transmission system. In the following, aspects for the converter topology selection are discussed.
Besides high efficiency, the most important requirement, the transition time between zero and maximum field current must meet a dynamics requirement (e. g. 100 msec) to provide a sufficiently quick torque rise on vehicle level. Another challenge is to offer not only a single operating point but a range of rotor currents between 2 A up to 17 A.
For the first requirement (high efficiency) the power electronics are operated in zero voltage switching (ZVS) mode by using a resonant or phase shift converter topology.
To meet the dynamics requirement, the secondary voltage must be increased above the stationary voltage level. This can be accomplished by the resonant converter topology. This converter type is known to have a flat voltage frequency response curve, see Fig. 3. The flat characteristic means that low secondary voltage and current values cannot be supported by this topology.

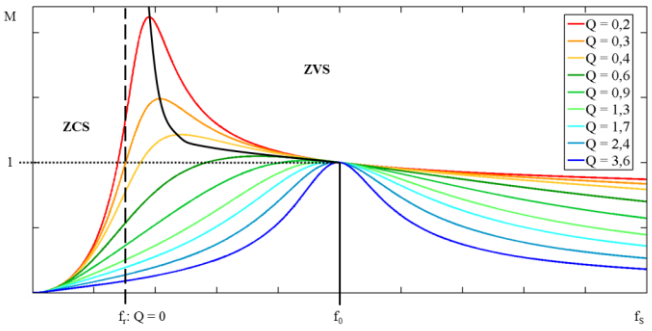

Fig. 3: Typical, flat voltage frequency response of a resonant converter depending on the Q-factor

The requirement of a wide field winding current range calls for a phase shift converter, which on the other hand cannot supply the maximum current and current rise time requirements due to voltage losses at the comparatively big stray inductance value of the rotary transformer.

To sum up, none of the known converter types meets all requirements. Yet, a full bridge resonant converter that is operated flexible (e. g. phase shift and burst modes) can be applied successfully.

III. Rotating Transformer

A. Tranformer geometry

For choosing the geometry it is necessary to regard the transmitted power to remain constant when the shaft is rotating. By [6] and [7], it is possible with the basic shapes which are illustrated in Fig. 4.

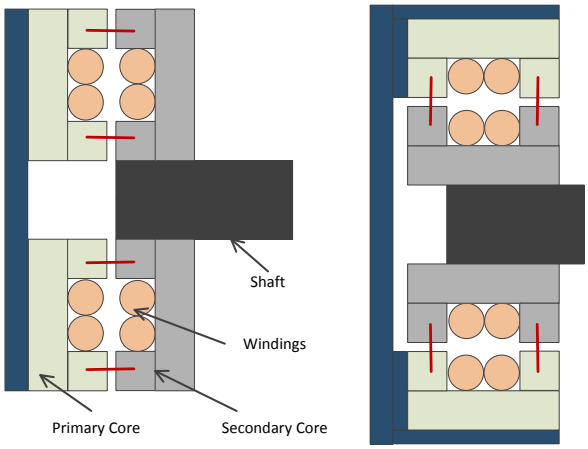

Fig. 4: Left: axial version (pot cores); right: radial version

As the air gap length at the pot core version and the air gap cross-section at the radial version vary due to axial movement, these geometries are only partially suitable for EESM, which requires other shapes. In Fig. 5 two versions are shown in detail. These core forms avoid axial motion insensitivity due to an overlap of the cores.

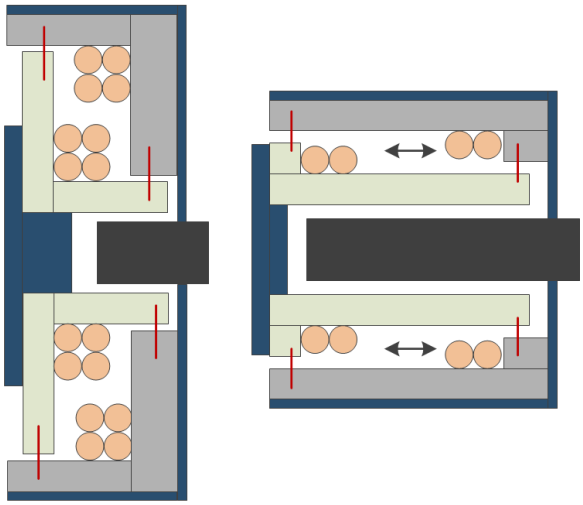

Fig. 5: Left: version 1; right: version 2

B. Core size

The transformer´s size is based on the one hand on the slot size, which can be calculated via equation (1) and on the other hand using the core´s length and the core´s cross-section.

$$A_w = \frac{N \cdot I}{J \cdot k_F} \tag{1}$$

By means of the maximum magnetic flux which flows through the core, it is possible to calculate the cross-section area. The core´s length depends, on the other hand, on the slot size. Assuming a sinusoidal input and a homogeneously distributed flux density is thus calculated from the formulas (2) and (3) giving the equation (4).

$$\Phi = \int B \, dA \tag{2}$$

$$\Phi = -\int U(t) \, dt \tag{3}$$

$$A_{min} = \frac{U}{\sqrt{2}\pi \cdot f \cdot N \cdot B_{max}} \tag{4}$$

Alternatively it is possible to calculate the necessary cross-section directly from the transportable power by transposing the formula (4) to U as well as the formula (1) to I and multiply both terms by equation (5).

$$A_{min} = \frac{P_{trans}}{\sqrt{2}\pi \cdot B_{max} \cdot A_w \cdot k_F \cdot J \cdot f} \tag{5}$$

C. Optimizing the installation space

As the transformer´s size depends on the one hand on (1) ~N and on the other hand on (4) $\sim N^{-1}$ as well as $\sim f^{-1}$, it is necessary to find a size optimum. Therefore it is essential to determine the total weight out of the core´s and winding´s geometry. At the same time constraints must be adhered so that only the permitted operating points are remaining. In Fig. 6, the geometrical construction of version 1, the radii and the lengths of the minimum cross-sectional core and the slot´s size is shown. By (1) the slot´s width and height can be calculated, whereas according to [8] it is recommendable to choose a wide slot with and a low height to avoid slot´s cross-leakage. These help to determine and to compare the total volume and by means of the corresponding material mass density the total weight, as shown in Fig. 7.

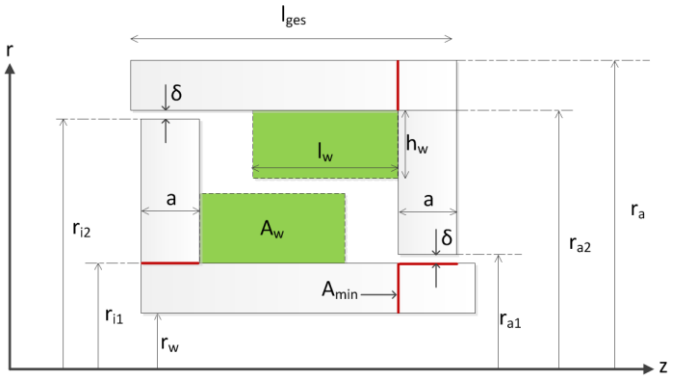

Fig. 6: Geometric parameters for the calculation of core version 1

TABLE II. GEOMETRICAL PARAMETERS OF FIG. 5

r_W, r_{i1}, r_{i2}, r_{a1}, r_{a2}, r_a	Radiuses of the different core parts
A	Length of limbs
l_{ges}	Length of core
Δ	Length of air gap
h_w	Height of the winding area F
l_w	Width of the winding area F
A_{min} (red line marker)	Minimal core cross-section Area
A_w	Winding cross-section Area

As expected, the weight decreases with increasing frequency. Depending on the number of turns per unit length, a minimum of weight for one frequency is achieved. As space constraints, such as a maximum available length and outer radius must be observed and core material thicknesses must not be exceeded, there are only the marked points feasible at all. The green highlighted marker shows the lightest version, which allows an operating frequency of at least 80 kHz at a secondary number of turns of 3 and a maximum flux density of 0.2 T by using ferrite.

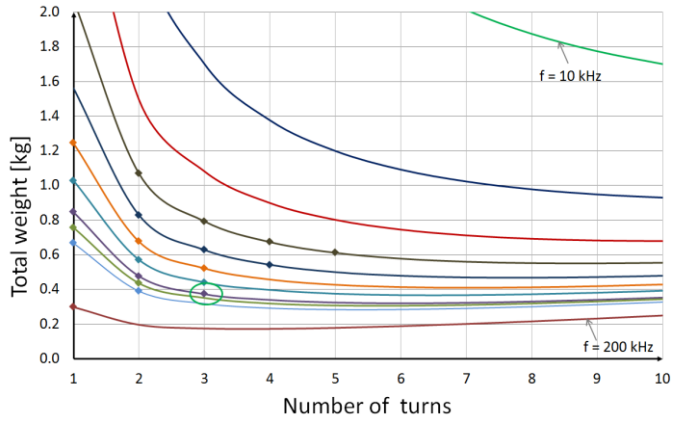

Fig. 7: Weight calculation of core version 1 related to secondary side in dependence of frequency

IV. SIMULATION AND CALCULATION

A. Reluctance Model

Usually, the first statements about the transmission behaviour ensue by means of the electrical T-Equivalent circuit after having calculated the inductances. These are either calculated from the reluctances or by means of the numerical calculation, whereas the latter provides according to [6] the most accurate results, but it is also the most computationally intensive one.

In order to estimate the transmitted power through the air gap in advance and to avoid unnecessary FEM calculations, the reluctance model was directly simulated with the program SimulationX without determining the inductors.

For calculating a magnetic resistance, formula (6) is basically applied. Along with it, the cross-section A which is floated by field lines, the length ℓ of the field lines as well as the material dependent permeability μ_r have to be known.

$$R_{mag} = \frac{l}{\mu_0 \cdot \mu_r \cdot A} \qquad (6)$$

In order to achieve accurate values, the Schwarz-Christoffel Transformation is preferred in [9], whose application is, however, as computationally intensive as the FEM method. A useful simplification is shown in [10], where the magnetic circuit is divided into sections and thereby a discrete model is generated. Regarding the verification, a model for the pot core variation was created previously which is shown in Fig. 8.

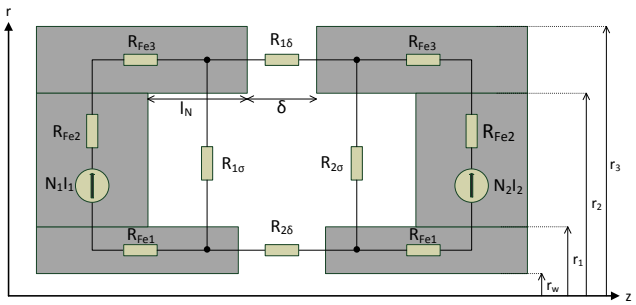

Fig. 8: Reluctance Model (Pot Core)

The air gap resistances were calculated with the equations (7), (8) and (9).

$$R_{1\delta} = \frac{\delta}{\mu_0 \cdot (r_3{}^2 - r_2{}^2) \cdot \pi} \qquad (7)$$

$$R_{2\delta} = \frac{\delta}{\mu_0 \cdot (r_1{}^2 - r_w{}^2) \cdot \pi} \qquad (8)$$

$$R_{1\sigma} = R_{2\sigma} = \frac{\ln\left(\frac{r_2}{r_1}\right)}{\mu_0 \cdot 2\pi \cdot \left(\frac{\delta}{2} + l_N\right)} \qquad (9)$$

For the simulation, the cores PCH 70 x 14.5 from EPCOS were used. In this case, a power transmission of 1kW was calculated using the parameter set in table III.

B. *Finite elements method (FEM)*

For the calculation of the primary and leakage inductances the ANSYS Maxwell program was used, which is based on FEM. Thereby, it is possible to determine the inductors very accurately which can help to optimize the transmission in relation to the resonant converter. The inductors for the T-equivalent circuit are calculated with [5] according to the magnetic flux and the coil current, based on one turn, with the formulas (10), (11) and (12), whereas $L_{1\sigma 0} = L_{2\sigma 0}$ is to be applied at identical coils.

$$L_{h0} = \frac{\Phi_2}{I_1} = \frac{\Phi_1}{I_2} \qquad (10)$$

$$L_{1\sigma 0} = \frac{\Phi_1 - \Phi_2}{I_1} \qquad (11)$$

$$L_{2\sigma 0} = \frac{\Phi_2 - \Phi_1}{I_1} \qquad (12)$$

When setting up the transmission system via pot core at a EESM you can only expect a change of the air gap length δ, however no missaligement of the cores. In this case, it is possible to take advantage of the symetry and to calculate in 2D as shown in Fig. 9.

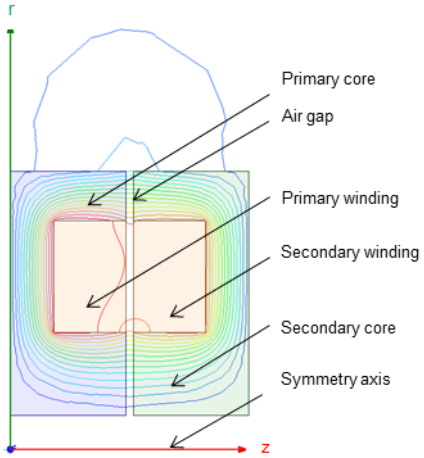

Fig. 9: Pot Core FEM Simulation

In Fig. 10 you can see the calculated and measured inductances, depending to the air gap´s length δ.

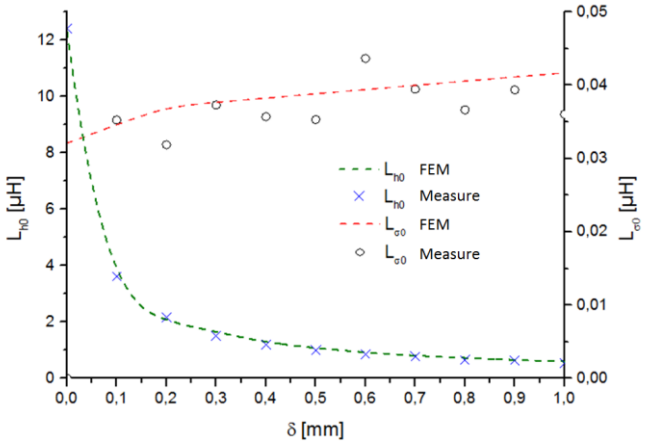

Fig. 10: Calculated and measured inductances

V. VERIFICATION

A first construction was realised as an axial version, built with N22 ferrite pot cores PCH 70 x 14.5 ([11]). S.396), shown in Fig. 11. The core size was previously determined with equation (4). The transferable power via the air gap was calculated with a reluctance model in SimulationX.

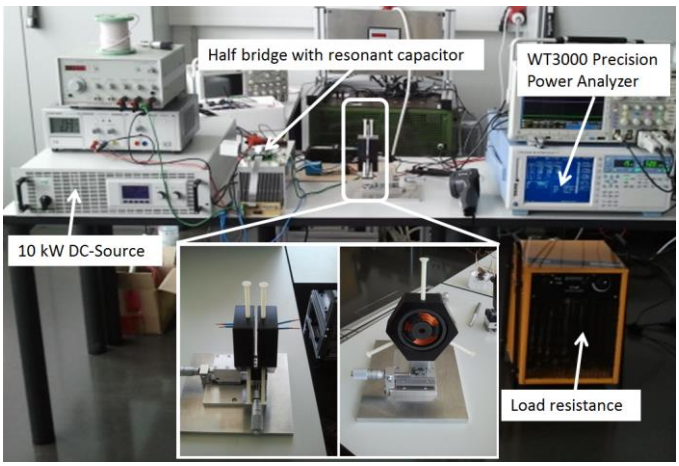

Fig. 11: Test setup

To verify the calculated inductors experimentally, the inductive power transmitter was operated with a sinusoidal source idling as well as short-circuited. The inductances were calculated with the formulas (13) - (17) by means of the measured currents and voltages.

<u>No-load condition</u>

$$U_1 = L_1 \cdot \omega \cdot I_1 \qquad (13)$$

$$U_2 = L_h \cdot \omega \cdot I_1 \qquad (15)$$

$$L_{1\sigma} = L_1 - L_h \qquad (17)$$

<u>Shorted</u>

$$L_2 = \frac{I_1}{I_2} \cdot L_h \qquad (14)$$

$$L_{2\sigma} = L_2 - L_h \qquad (16)$$

The inductors, calculated and measured, compared in Fig. 10 coincide with the measurement´s accuracy.

For the power transmission, a simple controlled resonant circuit was built consisting of a DC source, a half-bridge, a series resonance capacitor and the inductive transformer. In this case, a power of 1 kW was transferred at a transformer efficiency of 97.6 % through an air gap of 1mm. Previously, a power transmission of 1 kW was calculated with an estimated transformer´s efficiency of 98 % using the same configuration. The exact parameters of the experimental setup are shown in table III.

TABLE III. PARAMETERS OF THE TEST SETUP

Load resistance R_L	6.33 Ω
Resonance capacitor C	1.2 µF
Number of windings N_1=N_2 (litz wire, I_{max} = 20 A)	10
Length of air gap δ	1 mm
Operating frequency f	20 kHz
Resonance frequency f_0	18 kHz

VI. CONCLUSION

The inductive transformer´s design was verified with a construction, consisting of available pot cores. The calculated values agreed with the measured results. Thus, the next step is to expound and produce one of the above mentioned core geometries according to Fig. 5, for installation in an EESM.

REFERENCES

[1] J. Santiago, H. Bernhoff, B. Ekergard, S. Eriksson, S. Ferhatovic, R. Waters, M. Leijon, Electrical Motor Drivelines in Commercial All-Electric Vehicles: A Review, IEEE Transactions on vehicular technology, vol. 61, no. 2, February 2012.

[2] S. Thiele, Drehzahlstellbare, bürstenlose erregte Synchronmaschine mit integriertem Erregertransformator, Darmstadt, 1983.

[3] R. Fischer, Elektrische Maschinen, Hanser Verlag, 2009

[4] D. Ludois, „Capacitive Power Transfer of Rotor Field Current in Synchronous Machines,“ in Energy Conversion Congress and Exposition (ECCE) IEEE, 2011.

[5] D. Kürschner, Methodischer Entwurf toleranzbehafteter induktiver Energieübertragungssysteme, Aachen: Shaker Verlag, 2010.

[6] J.P.C. Smeets, D.C.J. Krop, J.W. Jansen, M.A.M. Hendrix, E.A. Lomonova, „Optimal Design of a Pot Core Rotating Transformer” in Energy Conversion Congress and Exposition (ECCE) IEEE, 2010.

[7] J. Legranger, G. Friedrich, S. Vivierl, J.C. Mipo, „Comparison of Two Optimal Rotary Transformer Design for Highly Constrained Applications“ in Electric Machines & Drives Conference, 2007. IEMDC '07. IEEE International (Volume:2)´

[8] Richter R.: Elektrische Maschinen Erster Band Allgemeine Berechnungselemente Die Gleichstrommaschine. Basel und Stuttgart: Birkhäuser Verlag 1967

[9] A. Balakrishnan, W. T. Joines, T. G. Wilson, Air-Gap Reluctance and Inductance Calculations for Magnetic Circuits Using a Schwarz–Christoffel Transformation in IEEE TRANSACTIONS ON POWER ELECTRONICS, VOL. 12, NO. 4, JULY 1997

[10] Kallenbach, Eick, Quendt, Ströhla, Feindt und Radler, Elektromagnete, Vieweg+Teubner Verlag, 2012

[11] Data Book 2013 „Ferrites and Accessories“ EPCOS AG. 2012